9986 *Inorg. Chem.* **2009**, *48*, 9986–9988
DOI: 10.1021/ic9015977

Inorganic Chemistry
Communication

Nitric Oxide Chemisorption in a Postsynthetically Modified Metal−Organic Framework

Michael J. Ingleson, Romain Heck, Jamie A. Gould, and Matthew J. Rosseinsky*

Department of Chemistry, University of Liverpool, Liverpool L69 7ZD, U.K.

Received August 10, 2009

Postsynthetic metal−organic framework (MOF) derivatization introduces accessible secondary amine functionalities that react with nitric oxide (NO) to form *N*-diazenium diolates. This is in contrast to the parent MOF that binds NO essentially irreversibly at open metal coordination sites.

One of the features provoking interest in porous metal−organic framework (MOF) materials is the possibility of postsynthetic transformations.[1−9] This methodology is developing into a powerful technique enabling the controlled modification of the chemical and physical properties of the pore environment using simple and predictable chemical reactions. Most importantly, this approach allows access to materials containing functionalities incompatible with conventional MOF synthetic methodologies. In this paper, postsynthetic transformation of a MOF by diamine grafting onto unsaturated metal centers introduces accessible secondary amine functionalities;[10,11] a subsequent reaction with nitric oxide (NO) generates a new organic species of relevance to NO storage. The controlled delivery of NO is important for numerous medical applications,[12] and porous materials have enabled notable advances in this field.[13−17] However, these materials are often limited by poor reversibility, or by an undesirably rapid release of NO. Our approach utilizes a two-step postsynthetic transformation of a MOF to generate *N*-diazenium diolates (a "masked" version of NO)[18,19] inside a microporous material. *N*-Diazenium diolate formation inside a porous material is conceptually attractive because of (i) the strong nature of NO binding to secondary amine sites (irreversible until triggered) and (ii) the ability of H_2O to act as an efficient trigger for NO release.

The synthesis of a MOF containing an accessible secondary amine was initiated by postsynthetic transformation of the extensively studied HKUST-1 (Figure 1).[20−22] Amine functionalization of HKUST-1 has been previously reported with the synthesis of $[Cu_3btc_2(pyridine_3)]_\infty$, where each Cu now binds a single pyridine molecule.[20] For further functionalization, pyridyl groups are particularly appealing because of the strong irreversible binding of the sp^2 hybridised N to Cu. Thus, in a related manner, we targeted impregnation into HKUST-1 of the bifunctional amine, 4-(methylamino)-pyridine (4-map; Figure 1), which possesses a N sp^2 lone pair and a 2° amine functionality for reaction with NO. Postsynthetic transformation is essential as attempts to directly produce 4-map-loaded HKUST-1 solvothermally failed, with amine-incorporated HKUST-1 not accessible using standard conditions.[23]

*To whom correspondence should be addressed. E-mail: m.j.rosseinsky@liverpool.ac.uk.

(1) Ingleson, M. J.; Barrio, J. P.; Bacsa, J.; Dickinson, C.; Park, H.; Rosseinsky, M. J. *Chem. Commun.* **2008**, 1287.
(2) Wang, Z.; Cohen, S. M. *Angew. Chem., Int. Ed.* **2008**, *47*, 4699.
(3) Morris, W.; Doonan, C. J.; Furukawa, H.; Banerjee, R.; Yaghi, O. M. *J. Am. Chem. Soc.* **2008**, *130*, 12626.
(4) Goto, Y.; Sato, H.; Shinaki, S.; Sada, K. *J. Am. Chem. Soc.* **2008**, *130*, 14354.
(5) Burrows, A. D.; Frost, C. G.; Mahon, M. F.; Richardson, C. *Angew. Chem., Int. Ed.* **2008**, *47*, 8482.
(6) Seo, J. S.; Wand, D.; Lee, H.; Jun, S. I.; Oh, J.; Jeon, Y.; Kim, K. *Nature* **2000**, *404*, 982.
(7) Costa, J. S.; Gamez, P.; Black, C. A.; Roubeau, O.; Teat, S. J.; Reedijk, J. *Eur. J. Inorg. Chem.* **2008**, 1551.
(8) Ingleson, M. J.; Barrio, J. P.; Guilbaud, J.-B.; Khimyak, Y. Z.; Rosseinsky, M. J. *Chem. Commun.* **2008**, 2680.
(9) Kawamichi, T.; Kodama, T.; Kawano, M.; Fujita, M. *Angew. Chem., Int. Ed.* **2008**, *47*, 8030.
(10) Demessence, A.; D'Alessandro, D. M.; Foo, M. L.; Long, J. R. *J. Am. Chem. Soc.* **2009**, *131*, 8784.
(11) Hwang, Y. K.; Hong, D.-Y.; Chang, J.-S.; Jhung, S. H.; Seo, Y.-K.; Kim, J.; Vimont, A.; Daturi, M.; Serre, C.; Ferey, G. *Angew. Chem., Int. Ed.* **2008**, *47*, 4144.
(12) Keefer, L. K. *Nat. Mater.* **2003**, *2*, 357.
(13) Xiao, B.; Wheatley, P. S.; Zhao, X.; Fletcher, A. J.; Fox, S.; Rossi, A. G.; Megson, I. L.; Bordiga, S.; Regli, L.; Thomas, M.; Morris, R. E. *J. Am. Chem. Soc.* **2007**, *129*, 1203.
(14) Wheatley, P. S.; Butler, A. R.; Crane, M. S.; Fox, S.; Xiao, B.; Rossi, A. G.; Megson, I. L.; Morris, R. E. *J. Am. Chem. Soc.* **2006**, *128*, 502.
(15) McKinlay, A. C.; Xiao, B.; Wragg, D. S.; Wheatley, P. S.; Megson, I. L.; Morris, R. E. *J. Am. Chem. Soc.* **2008**, *130*, 10440.
(16) Bonino, F.; Chavin, S.; Vitillo, J. G.; Groppo, E.; Agostini, G.; Lamberti, C.; Dietzel, P. D. C.; Prestipino, C.; Bordiga, S. *Chem. Mater.* **2008**, *20*, 4957.
(17) Morris, R. E.; Wheatley, P. S. *Angew. Chem., Int. Ed.* **2008**, *47*, 4966.
(18) Parzuchowski, P. G.; Frost, M. C.; Meyerhoff, M. E. *J. Am. Chem. Soc.* **2002**, *124*, 12182.
(19) Hrable, J. A.; Keefer, L. K. *Chem. Rev.* **2002**, *102*, 1135.
(20) Chui, S. S.-Y.; Lo, S. M.-F.; Charmant, J. P. H.; Orpen, A. G.; Williams, I. D. *Science* **1999**, *283*, 1148.
(21) Cychosz, K. A.; Wong-Foy, A. G.; Matzger, A. J. *J. Am. Chem. Soc.* **2008**, *130*, 6938.
(22) Schlichte, K.; Kratzke, T.; Kaskel, S. *Microporous Mesoporous Mater.* **2004**, *73*, 81.
(23) See the Supporting Information.

 Published on Web 10/01/2009

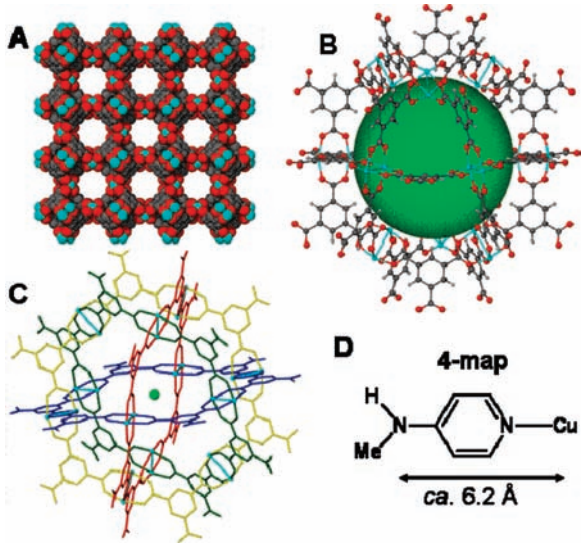

Figure 1. (A) Space-filling diagram of the HKUST-1 framework (HKUST-1 = Cu_3btc_2, btc = 1,3,5-benzenetricarboxylate) showing the larger pore windows.[20] (B) Cubeoctahedron pore, a sphere of 15 Å inserted to emphasize the pore space. Color code: O, red; C, gray; Cu, cyan. (C) Four intersecting rings that define the large cubeoctahedron pore. Each Cu_2 paddlewheel (cyan) projects one nonbridging binding site toward the center of the pore (green sphere). (D) Approximate dimensions of 4-map.

4-map was successfully introduced into HKUST-1 using vapor-phase diffusion at 413 K, producing material of the general formula $[Cu_3(btc)_2(4\text{-map})_x(H_2O)_y]_\infty$, termed FW($x$) ($x$ = percentage of Cu with 4-map bound). The ligand-exchange reaction is accompanied by the expected color change from light blue to green, indicative of pyridyl N coordination to Cu.[20] The extended framework structure was maintained throughout, with closely comparable powder X-ray diffraction (pXRD) patterns observed before and after loading (Figure 2). Precise amine loading levels were determined by a combination of elemental microanalysis, thermogravimetric analysis (TGA), and solution NMR spectroscopy (postframework dissolution).[23] The ^{1}H NMR spectrum of the dissolved framework comprised only resonances attributable to btc and 4-map in the expected ratios. Materials with a range of Cu:amine stoichiometries were accessible up to the maximum of three 4-map per empirical unit [FW(x), x = 32−97%] equivalent to one amine per Cu. Prolonged soaking of FW(x) materials (in H_2O, MeOH, EtOH, or DMF) resulted in no loss of adsorbed 4-map (by elemental analysis and solution NMR of the filtrate), confirming the robustness of the amine−Cu bond.

The adsorbed 4-map could feasibly be present as either a chemisorbed guest (coordinatively bound to Cu), a physisorbed species, or a mixture of the two forms. To ensure the removal of any physisorbed 4-map, the material, after amine loading, was heated (393 K) *in vacuo* (1×10^{-3} Torr). This resulted in a small quantity of 4-map subliming out of the framework (by solution NMR analysis on isolated solid). Subsequent prolonged heating under high vacuum (1×10^{-7} Torr) produced no further amine loss (by in situ gravimetric analysis),[23] strongly suggesting that all remaining 4-map is present as chemisorbed, Cu-bound species. Concomitant with the desorption of physisorbed 4-map during vacuum treatment is the removal of all H_2O from the pore space (by microanalysis). The loss of H_2O from the framework is fully reversible with exposure of the dehydrated material to moist air, resulting in the regeneration of the H_2O-solvated material. All functionalized materials discussed herein have had physisorbed 4-map and H_2O removed *in vacuo* (393 K 18 h) and stored under argon.

The 4-map-impregnated HKUST-1, FW(60%), was nonporous to N_2 (to 1 bar at 77 K), in contrast to unfunctionalized HKUST-1.[13] The porosity in HKUST-1 is defined by three distinct cavities interconnected by two types of pore windows.[24] For chemisorption of 4-map to the Cu coordination sites, the larger pore window and the largest cavity are of key significance. The larger pore window in HKUST-1 (Figure 1A) has an approximate diameter of 8 Å, sufficient for 4-map diffusion. The Cu-bound nonbridging ligands do not project directly into the pore window, but rather they are oriented into the larger cubeoctahedron pores. These cubeoctahedron pores are defined by four "rings", each comprising six Cu_2 paddlewheels connected by btc ligands, generating a pore-wall environment containing 12 paddlewheels. Crucially, for porosity after amine binding, each nonbridging ligand-binding site projects directly into the center of the pore (Figure 1B,C). A comparison of the cross-pore Cu···Cu distance (~16 Å) to the dimensions of 4-map reveals that even at low loading levels (e.g., 50% Cu atoms binding 4-map) this pore is sterically crowded, with the Cu-bound 4-map N(H)Me groups converging at the pore center, forcing them into close spatial proximity. This is consistent with the observed nonporosity of FW(60%) at 77 K. Despite the observed nonporous nature of FW(60%) to N_2 (albeit at 77 K) combined elemental microanalysis and TGA indicated reversible H_2O sorption (at 293 K),[23] intrinsically implying a degree of porosity to small molecules at 293 K. Thus, the ability of FW(60%) to adsorb and react with NO was investigated. Exposing FW(60%) to NO (2 bar, 72 h, 293 K) resulted in the formation of *N*-diazenium diolate functionalities, unambiguously identified by the appearance of diagnostic stretching bands in the IR spectrum (Figure 2, at 1225−1210, 1187−1155, and 1131−1129 cm^{-1}).[19] Elemental microanalysis confirmed the sorption of NO, forming a material consistent with the empirical formula $Cu_3(btc)_2(4\text{-map})_{1.8}(NO)_{0.7}$, termed FW(60%)(NO-23%) where (NO-xx refers to the percentage of NO per Cu atom). The framework, after NO adsorption, is still crystalline, with pXRD confirming retention of the cubic framework structure of HKUST-1 (Figure 2). FW(60%)(NO-23%) is resistant to NO loss upon prolonged exposure to a vacuum, with no change in the elemental microanalysis precluding significant physisorbed NO. The absence of IR stretches corresponding to NO directly bound to Cu (at 1887 cm^{-1}) in FW(60%)(NO-23%) strongly suggests that *N*-diazenium diolate formation is the major mechanism of NO sorption operating in FW(60%). Thus, the postsynthetic modification of HKUST-1 with 4- map has generated a material with a new NO binding mode that is distinct to chemisorption at open metal sites (M ← NO) that operates in the parent MOF.[13]

The close proximity of amine groups in FW(60%) generates a prearranged reaction site where one amine can combine with two molecules of NO, producing the unstable protonated *N*-diazenium diolate.[19] Subsequent proton transfer to a proximal amine then forms the observed stable

(24) Chapman, K. W.; Halder, G. J.; Chupas, P. J. *J. Am. Chem. Soc.* **2008**, *130*, 10524.

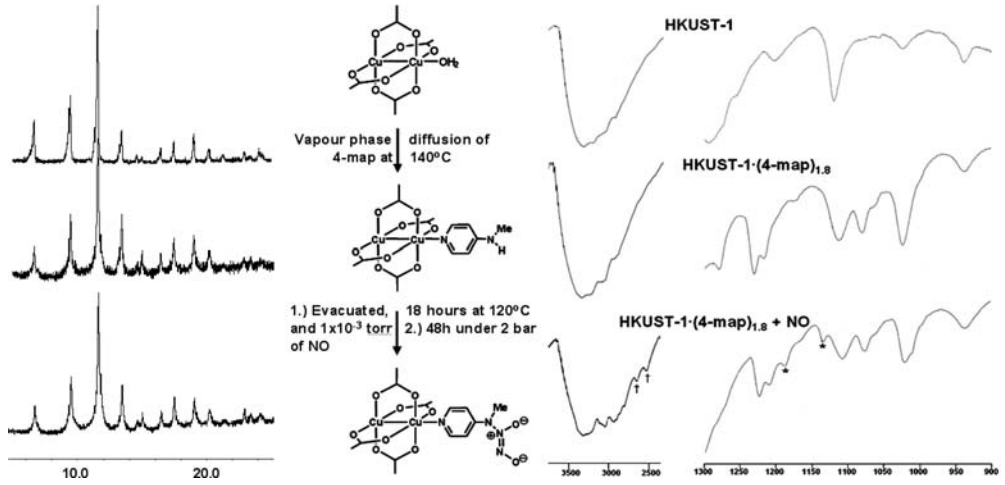

Figure 2. (Left) pXRD before and after each functionalization (2θ range = 5−25°). (Right) IR spectra (KBr disk) before and after each functionalization. * = *N*-diazenium diolate stretches at 1180 and 1129 cm^{-1}. The third expected stretch (1225−1210 cm^{-1}) is obscured by stretches associated with FW(60%). † = stretches associated with ammonium cations (2550−2700 cm^{-1}).

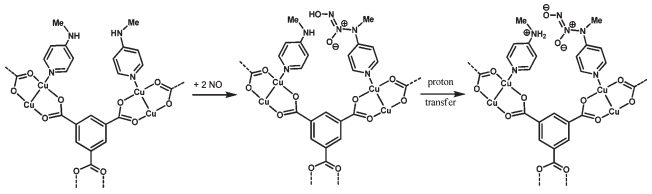

Figure 3. Simplified schematic of the prearranged reactive sites in the pores of FW(60%) that enable the production of *N*-diazenium diolate.

deprotonated *N*-diazenium diolate along with an ammonium cation (Figure 3). Ammonium cation N−H stretches are indeed observed in the IR spectrum after NO exposure (Figure 2, 2550−2700 cm^{-1} region), consistent with this mechanism. The substoichiometric conversion of amine to *N*-diazenium diolate (theoretical maximum of 1:1 NO/4-map) is attributed to (i) pores inaccessible to NO and (ii) pores where two secondary amines are insufficiently close to enable concerted NO binding and deprotonation. In these latter pores, the unstable protonated *N*-diazenium diolates will decay back to their constituent parts upon removal of external NO. This hypothesis is indirectly supported by the fact that NO is adsorbed (by microanalysis) in the FW(32) 4-map-loaded framework but with minimal formation of *N*-diazenium diolate functionalities (by IR). Instead, the major NO adsorption vehicle is directly to the Cu sites, as was previously observed in unfunctionalized HKUST-1.[13] The lack of *N*-diazenium diolate formation observed for FW(32%) is most probably due to a low number of pores possessing two sufficiently proximal amines. The addition of external bases did not increase the yield of *N*-diazenium diolate, presumably because of solvated basic species being excluded (based on size) from entering the pore network. For the highest loaded material, x = 97%, there was no NO sorption by either mechanism, with complete pore blockage preventing NO uptake.

FW(60%)(NO-23%) is stable when stored under an inert atmosphere (by IR and microanalysis), confirming the thermal stability of the deprotonated *N*-diazenium diolate moiety. Exposure to an ambient atmosphere results in a gradual decrease in the IR stretches associated with *N*-diazenium diolate, with complete loss occurring over 5 days, implying that NO binding in FW(60%) is not irreversible. Encouraged by this result, FW(60%)(NO-23%) was suspended in deionized H_2O for 18 h. Analysis after framework isolation revealed not only the loss of all *N*-diazenium diolate functionalities but significant leaching of 4-map (by microanalysis).[20] Amine does not leach from FW(60%) under identical conditions; thus, 4-map loss is an attribute arising after NO exposure and *N*-diazenium diolate formation. We postulate that a byproduct formed during H_2O-triggered *N*-diazenium diolate decomposition of FW(60%)(NO-23%) effects Cu ← N_{py} dative bond breakage, facilitating amine desorption (HNO_2 or a related decomposition byproduct could feasibly protonate the pyridyl N sp^2 breaking the dative bond).[19] The H_2O solution was acidic after FW(60%)(NO-23%) soaking, confirming the production of acidic species fully consistent with this mechanism. This instability to H_2O severely limits the usefulness of these materials toward NO delivery, with reversible NO storage via *N*-diazenium diolates not compatible with metal−ligand dative bonds.

In conclusion, we have successfully impregnated a bifunctional amine into a porous material using coordinative bonding to metal centers. The introduced 2° amine functionalities perform two distinct roles inside the cavity, both of which are essential for the successful formation of *N*-diazenium diolates: (i) direct reaction with NO; (ii) deprotonation of an unstable intermediate. It is only the precise structural arrangement of amines inside the cavity that enables this reaction to proceed. The functionalized framework's response to NO is drastically different from that of the parent material. This is a rare example of the deliberate postsynthetic modification of a MOF altering the material's reactivity in a desirable and predictable manner.

Acknowledgment. Financial support was provided by EPSRC Grant EP/C511794.

Supporting Information Available: Experimental procedures and full characterization of all compounds. This material is available free of charge via the Internet at http://pubs.acs.org.